Inorganic Chemistry

Article

pubs.acs.org/IC

Influence of Symmetry on the Luminescence and Radiative Lifetime of Nine-Coordinate Europium Complexes

Nail M. Shavaleev,* Svetlana V. Eliseeva, Rosario Scopelliti, and Jean-Claude G. Bünzli*

École Polytechnique Fédérale de Lausanne, Institut des Sciences et Ingénierie Chimiques, Avenue Forel 2, BCH, CH-1015 Lausanne, Switzerland

Supporting Information

ABSTRACT: Homoleptic mononuclear nine-coordinate lanthanum(III) and europium(III) tris-complexes $[Ln(N^\wedge N^\wedge O)_3]\cdot nH_2O$ with two tridentate *N*-benzylbenzimidazole pyridine-2-carboxylates exhibit a rare C_3-symmetry of the lanthanide coordination polyhedron in the solid state, as confirmed by luminescence spectroscopy and by X-ray crystallography (the three N^N^O ligands are arranged "up−up−up" around the lanthanide ion). The symmetry, however, is changed to the more common C_1 upon dissolution of the complexes in dichloromethane, as revealed by luminescence spectroscopy (the three ligands are likely to be arranged "up−up−down"). The new europium complexes emit efficient ligand-sensitized metal-centered luminescence with excited-state lifetimes of 1.56−2.18 ms and quantum yields of 25−41% in the solid and in solution. The change of the symmetry from (a higher) C_3 to (a lower) C_1 alters the luminescence spectrum, shortens the radiative lifetime, and increases the luminescence efficiency of the europium complexes.

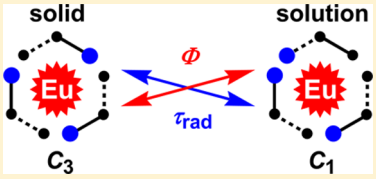

INTRODUCTION

Most trivalent lanthanide ions exhibit characteristic metal-centered line-like f−f luminescence with high color purity in the UV, visible, and near-infrared spectral ranges.[1−8] Although the f−f luminescence is long-lived, with a lifetime of up to milliseconds, it is usually not quenched by oxygen.[9]

The brightness of lanthanide luminescence, that is, the product of the luminescence quantum yield and the molar absorption coefficient (at the excitation wavelength), can be increased by many orders of magnitude by coordinating the lanthanide ion with chromophore ligands.[5,10−13] The ligands provide efficient light harvesting and ligand-to-lanthanide energy transfer and protect the lanthanide(III) from nonradiative deactivation.[5]

Upon coordination, mixing of ligand and lanthanide orbitals enhances the intensity of electric-dipole metal-centered Laporte-forbidden f−f transitions, especially when the coordination lowers the symmetry around the lanthanide.[1−3] Thus, the symmetry that the ligands define around the lanthanide ion in the complex determines the relative intensity of the emission bands and, therefore, both the luminescence color and the rate of radiative f−f transitions.[1−3,14,15]

The emissive lanthanide ions, in particular europium(III), are used as luminescent probes and sensors,[5] because the efficiency, the lifetime, and the fine structure of the f−f luminescence spectra are sensitive to the symmetry and the composition of the coordination sphere of the lanthanide.[1−5,11−15] Here, we report on rare mononuclear nine-coordinate lanthanide(III) complexes $[Ln(N^\wedge N^\wedge O)_3]$ that exhibit C_3-symmetry in the solid state but C_1-symmetry in solution and on the effect that this change of symmetry has on the luminescence of the europium(III) complexes.

RESULTS AND DISCUSSION

Synthesis. Two new tridentate monoanionic N^N^O ligands **HL1** and **HL2** have been prepared from 2-carboxaldehyde-6-hydroxymethylpyridine (Scheme 1).[16,17] The formation of a benzimidazole heterocycle[18] was followed by selective oxidation of pyridine-2-methanol first to carboxaldehyde with

Scheme 1. Synthesis of Ligands and Complexes[a]

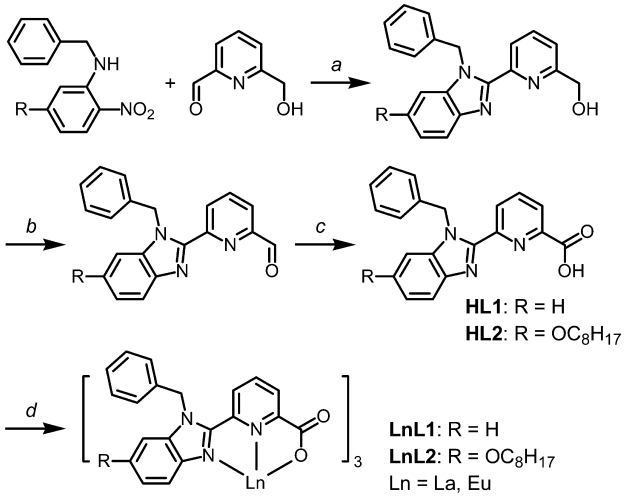

[a]Reaction conditions: (a) $Na_2S_2O_4$, 2-methoxyethanol/water or DMF/water, under nitrogen, 100−110 °C; (b) SeO_2, dioxane, under nitrogen, 110 °C; (c) H_2O_2, formic acid, under air, 0 °C; (d) $LnCl_3\cdot nH_2O$, NaOH, ethanol/water, under air, heating.

Received: July 16, 2015

DOI: 10.1021/acs.inorgchem.5b01580
Inorg. Chem. XXXX, XXX, XXX−XXX

SeO_2 and then to carboxylic acid with H_2O_2/formic acid.[19] The homoleptic lanthanum(III) and europium(III) tris-complexes $[Ln(Ligand)_3]\cdot nH_2O$ (n = 4, 5; Ln = La, Eu; Ligand = $L1^-$, $L2^-$; **LnL1** and **LnL2**) have been obtained by reacting a 3:3:1 molar ratio of ligand, NaOH, and $LnCl_3\cdot nH_2O$ in ethanol/water mixtures. All of the products are air- and moisture-stable solids. They have been characterized by elemental analysis, NMR spectroscopy, ESI TOF mass spectrometry, and X-ray crystallography. The n-octyloxy group in the benzimidazole heterocycle increases the solubility of ligand **HL2** and its complexes in organic solvents.

Molecular Structure of the Complexes LnL1. Figure 1 and Table 1 report the X-ray structure of $[La(L1)_3]\cdot CH_3CN$.

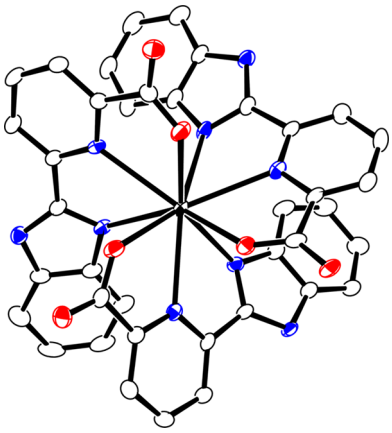

Figure 1. Structure of $[La(L1)_3]\cdot CH_3CN$ viewed down the triangular face (C_3 axis) of the tricapped trigonal prism (50% probability ellipsoids; one of the two independent molecules of the complex, the Λ isomer La(1), is shown; H atoms, benzyl groups, and cocrystallized acetonitrile molecule omitted; ORTEP). Heteroatoms: O, red; N, blue; La(1), black.

Table 1. Structure of $[La(L1)_3]\cdot CH_3CN$[a]

complex	bond lengths (Å) La−O	La−N(py)	La−N(b)	angles[b] (deg) py−b
$[La(L1)_3]$ (1)	2.448(3)	2.695(3)	2.737(3)	24.4
	2.452(3)	2.693(3)	2.735(4)	21.5
	2.459(3)	2.690(4)	2.755(3)	24.5
$[La(L1)_3]$ (2)	2.449(3)	2.705(3)	2.722(4)	16.4
	2.457(3)	2.688(4)	2.782(3)	26.3
	2.457(3)	2.705(3)	2.745(3)	22.2
average (2σ)	2.454(8)	2.696(13)	2.746(38)	23(6)
max − min	0.011	0.017	0.060	9.9

[a]Two independent molecules are present in the unit cell. Each row corresponds to one ligand. py = pyridine. b = benzimidazole. [b]The dihedral angles between the planes of pyridine and benzimidazole.

The structure contains two slightly different molecules (both are present as Λ and Δ isomers). The lanthanum ions are nine-coordinated by three deprotonated tridentate N^N^O ligands. Their coordination polyhedron is a distorted tricapped trigonal prism, with the N(py = pyridine) atoms in capping positions and in-plane with La^{III} (Figure 2). The La−La distance is long, 9.142(2) Å. The triangular faces of the prism are defined by O−O−O and N(b)−N(b)−N(b) atoms (b = benzimidazole). The three ligands are arranged "up−up−up" around the La^{III}, resulting in a complex with a distorted C_3-symmetry.

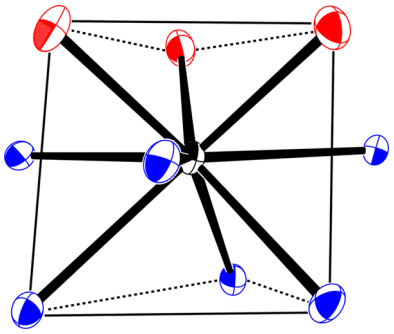

Figure 2. Coordination environment of La^{III} in $[La(L1)_3]\cdot CH_3CN$ viewed down the square face of the tricapped trigonal prism. Heteroatoms: O, red; N, blue; La(1), black.

The coordinated ligands are not planar, with the dihedral angles between pyridine and benzimidazole in the range 16.4−26.3°. The ligands are not equally strongly bonded to the metal ion. For a given ligand, the lanthanum−benzimidazole bond is the longest one with the widest variation. The bonding of the ligands was quantified by the bond-valence method,[20] wherein a donor atom j at a distance $d_{Ln,j}$ from the metal ion is characterized by a bond-valence contribution $\nu_{Ln,j}$:

$$\nu_{Ln,j} = e^{(R_{Ln,j} - d_{Ln,j})/b} \quad (1)$$

where $R_{Ln,j}$ are the bond-valence parameters for the interacting atoms (La−O, 2.148 Å; La−N, 2.261 Å)[21] and b is a constant (0.37 Å). The bond-valence sum (BVS) of the metal ion V_{Ln} is supposed to match its oxidation state,[20] if average bonds are standard:

$$V_{Ln} = \sum_j \nu_{Ln,j} \quad (2)$$

The BVS for the $[La(L1)_3]\cdot CH_3CN$ structure (3.03 and 3.07) is close to the expected value for La^{III} (3.00 ± 0.25) (Table 2).[20,21] The average contributions from the coordinating groups are in the expected order of affinity O, 0.44(1) > N(py), 0.31(1) > N(b), 0.27(3) (Table 2) and are within experimental error of those reported for the reference complexes **R1** (Chart 1).[17]

Table 2. Bond Valence Parameters of $[La(L1)_3]\cdot CH_3CN$[a]

complex	V_{Ln}	$\nu_{Ln,j}$[b] O	N(py)	N(b)
$[La(L1)_3]$ (1)	3.07	0.44(1)	0.31(0)	0.27(1)
$[La(L1)_3]$ (2)	3.03	0.44(1)	0.31(1)	0.27(4)
all data		0.44(1)	0.31(1)	0.27(3)

[a]Two independent molecules are present in the unit cell. [b]Bond-valence contribution with standard deviation 2σ averaged over the three ligands.

The X-ray structure of $[Eu(L1)_3]$ was of low quality (not shown), but it confirmed the connectivity, the presence of two independent molecules, and the C_3-symmetry of the complex. The long Eu−Eu distance in the structure (>9 Å) may minimize concentration quenching and may favor efficient luminescence of **EuL1**.

A review of the literature reveals that C_3-symmetry is rare for mononuclear tris-complexes $[Ln(N^\wedge N^\wedge O)_3]^{0/3-}$. Only two examples of C_3-symmetry but 32 examples of C_1-symmetry (where the three ligands are arranged "up−up−down") were

DOI: 10.1021/acs.inorgchem.5b01580
Inorg. Chem. XXXX, XXX, XXX−XXX

Chart 1. Reference Ligands and Complexes[a]

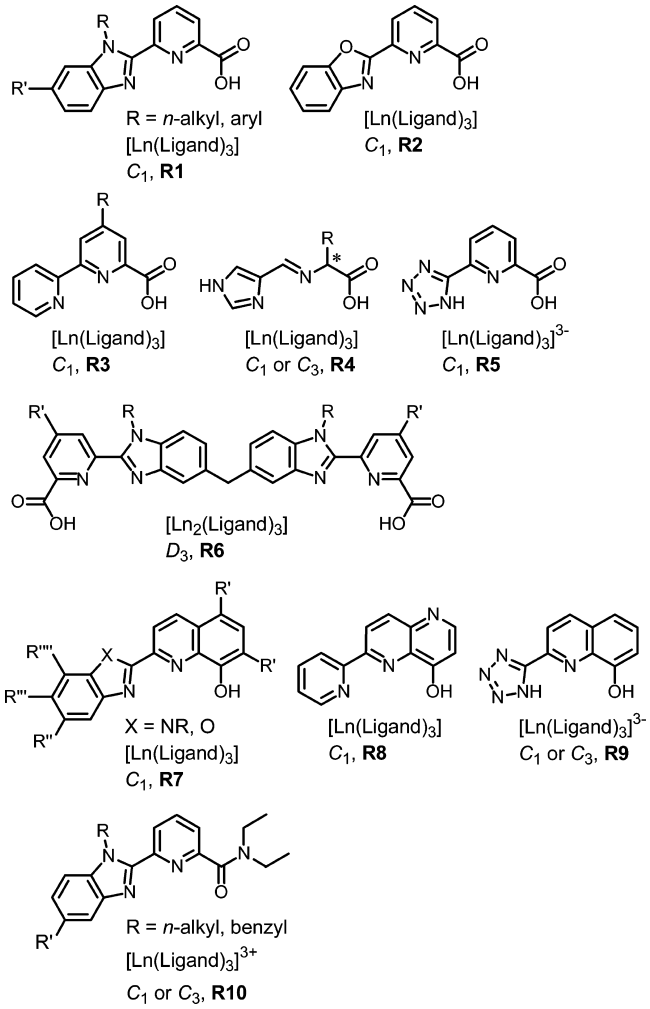

[a]The ligands bond by the set of N^N^O atoms with deprotonated carboxylate, phenolate, and tetrazolate groups. The composition and symmetry of the complexes are indicated. From the references: **R1**,[17] **R2**,[2] **R3**,[22] **R4**,[23] **R5**,[24] **R6**,[2] **R7**,[2] **R8**,[25] **R9**,[26] **R10**.[36]

reported for the structures of the reference complexes **R1**−**R5**[2,17,22−24] and **R7**−**R9**[2,25,26] (Chart 1).

Electronic States of the Ligands. The new ligands and their complexes exhibit electronic absorption transitions at wavelengths of less than 410 nm in organic solvents (Figure 3). The main composite absorption band with a maximum at 315−342 nm is assigned to the $\pi \rightarrow \pi^*$ transitions of the benzimidazole chromophore. From the ligands to the complexes,

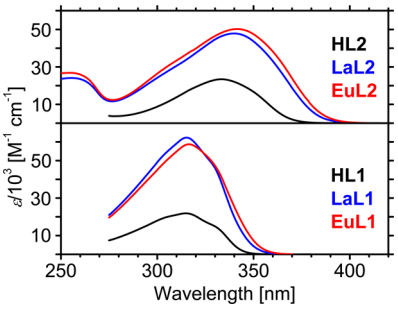

Figure 3. Absorption spectra of ligands (in DMSO) and complexes (**LnL1** in DMSO; **LnL2** in dichloromethane).

Table 3. Absorption Spectra of Ligands and Complexes[a]

compound	λ_{max}/nm (ε/10^3 M^{-1} cm^{-1})
HL1·H_2O	315 (22)
[La(L1)$_3$]·4H_2O	315 (62)
[Eu(**L1**)$_3$]·4H_2O	316 (59)
HL2·0.5H_2O	334 (23)
[La(L2)$_3$]·4H_2O[b]	340 (48), 256 (24)
[Eu(L2)$_3$]·5H_2O[b]	342 (50), 254 (27)

[a]See Figure 3. In DMSO at 298 K. Errors: λ_{max}, ±1 nm; ε, ±5%. [b]In dichloromethane.

its maximum red-shifts by up to 8 nm and its molar absorption coefficient increases from (22−23) × 10^3 M^{-1} cm^{-1} to (48−62) × 10^3 M^{-1} cm^{-1} (Table 3).

The ligand-to-lanthanide energy transfer often occurs mainly from the triplet state of the ligand.[1,2,27,28] Its efficiency depends on the overlap integral between the emission spectrum of the donor and the absorption spectrum of the acceptor and may be related to the energy gap between the ligand triplet state and the lanthanide receiving level(s).[1,28] The triplet-state energies of the coordinated ligands in lanthanum complexes (E_T) were determined from the zero-phonon transition in the phosphorescence spectra at 77 K to be 20 400 cm^{-1} for **LaL1** and 19 700 cm^{-1} for **LaL2** (Figure 4 and Table 4). These ligand

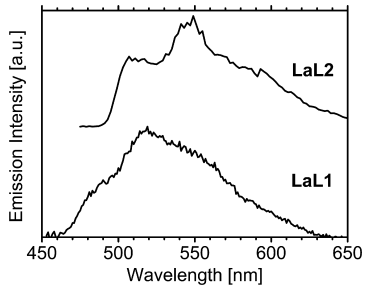

Figure 4. Phosphorescence spectra (corrected and normalized) of polycrystalline solid lanthanum complexes at 77 K.

Table 4. Phosphorescence of Lanthanum Complexes[a]

complex	E/10^3 cm^{-1} 0−0	0−1	Δ
[La(L1)$_3$]·4H_2O	20.4	19.3	1.1
[La(L2)$_3$]·4H_2O	19.7	18.2	1.5

[a]See Figure 4. In polycrystalline solid at 77 K. Error: ±200 cm^{-1}.

triplet states have sufficiently high energy for exothermic energy transfer to the Eu^{III} excited states[29] Eu($^5D_1$) at 19 000 cm^{-1} and Eu($^5D_0$) at ∼17 230 cm^{-1}.

The electron-donor *n*-octyloxy group in the benzimidazole heterocycle red-shifts both the absorption maximum by 1800−2400 cm^{-1} (19−26 nm) and the triplet state by 700 cm^{-1} from **HL1**/**LnL1** to **HL2**/**LnL2** by generating intraligand benzimidazole-centered "alkoxy"-to-imine charge-transfer transition.

Europium Luminescence. Upon excitation with UV and visible light, the new europium complexes emit characteristic red luminescence with a line-like spectrum in the range 575−710 nm due to the metal-centered $^5D_0 \rightarrow {}^7F_J$ ($0 \rightarrow J$, J = 0−4) transitions (Figure 5).[3] The emission spectra are independent of the excitation wavelength. The excitation spectra correspond to the ligand absorption transitions, thereby confirming

DOI: 10.1021/acs.inorgchem.5b01580
Inorg. Chem. XXXX, XXX, XXX−XXX

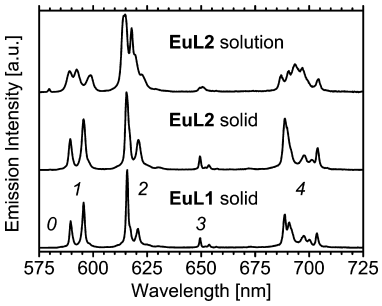

Figure 5. Luminescence spectra (corrected and normalized) of the europium complexes displaying the $^5D_0 \rightarrow {}^7F_J$ (J = 0−4) transitions at 298 K in the polycrystalline solid and in dichloromethane solution; λ_{exc} = 330 nm; emission slit: 0.2 nm.

ligand-to-europium energy transfer (Figure S1 in the Supporting Information). The new europium complexes do not exhibit ligand-centered fluorescence and phosphorescence.

High-resolution excitation scans over the $^5D_0 \leftarrow {}^7F_0$ transition of the polycrystalline solid complexes at 298 K exhibit one asymmetrical line with full width at half height (fwhh) of 9 cm^{-1} and maximum at 17 236 cm^{-1} for **EuL1** or 17 232 cm^{-1} for **EuL2** (Figure 6). Upon cooling to 10 K, the

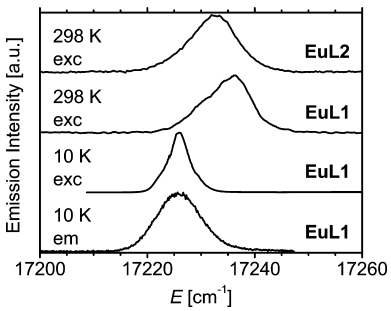

Figure 6. High-resolution excitation (exc) and emission (em) spectra of the $^5D_0 \rightarrow {}^7F_0$ transition of the polycrystalline solid europium complexes with 1 Å bandpass at 298 K and 10 K. The emission (for the excitation spectra) was monitored at the $^5D_0 \rightarrow {}^7F_2$ transition at 610−620 nm.

$^5D_0 \leftarrow {}^7F_0$ excitation transition for **EuL1** becomes narrower (fwhh = 4.4 cm^{-1}) and shifts to 17 226 cm^{-1}, but it remains asymmetrical, while the $^5D_0 \rightarrow {}^7F_0$ emission transition at 10 K displays a symmetrical broad line at 17 226 cm^{-1} with a fwhh of 9.8 cm^{-1} (Figure 6). A single sharp symmetrical line is expected for the electronic transition between the $^5D_0$ and $^7F_0$ levels of Eu^{III} in each unique coordination environment, provided that the transition is allowed by symmetry. The observed asymmetry of the $^5D_0 \leftarrow {}^7F_0$ excitation transition for the polycrystalline solids may arise from the presence of two nearly identical coordination environments of Eu^{III} (as confirmed by the X-ray analysis), from the variation in the conformation of (benzyl groups of the) organic ligands, and from defects in the microcrystals.[3]

The X-ray structures reveal that **LnL1** in single crystals have C_3-symmetry (Figures 1 and 2). Luminescence spectroscopy indicates that **EuL1** and **EuL2** in polycrystalline solids have C_3-symmetry also. The corrected emission spectra of the polycrystalline complexes **EuL1** and **EuL2** are similar (Figure 5). The emission intensity is fairly equally distributed among three main transitions (Table 5), the magnetic-dipole $^5D_0 \rightarrow {}^7F_1$ (22−24%), the hypersensitive $^5D_0 \rightarrow {}^7F_2$ (33−35%), and $^5D_0 \rightarrow {}^7F_4$ (38%), a situation typical of C_3-symmetry (see Figures 1 and 2).[3,23,30]

The crystal field splitting (Table 6) reveals 1, 2, 2 (or 2 + 1 shoulder), and at least 5 (or 4 + 1 shoulder) components for the $^5D_0 \rightarrow {}^7F_J$ transitions for J = 0, 1, 2, and 4. It is nearly in line with predictions for C_3-symmetry (1, 2, 3, and 6 components for J = 0, 1, 2, and 4),[3,30] except for the very weak intensity of the 0 → 0 transition, which is allowed in C_3 by symmetry-governed selection rules. The emission spectra of the polycrystalline **EuL1** and **EuL2** are almost consistent with a higher than C_3-symmetry in the same trigonal class, that is, with D_3-symmetry (0, 2, 2, and 4 transitions predicted for J = 0, 1, 2, and 4).[3]

High-resolution emission spectra of $^5D_0 \rightarrow {}^7F_1$ and $^5D_0 \rightarrow {}^7F_2$ transitions of polycrystalline **EuL1** at 10 K exhibit more components than would be expected for C_3-symmetry (Figure S2 in the Supporting Information), because of the reasons given above to explain the asymmetric $^5D_0 \leftarrow {}^7F_0$ excitation transition (Figure 6).

The emission spectrum of **EuL2** radically changes in going from the solid state to dichloromethane solution, indicating a change in the coordination environment of europium (Figure 5). In solution, the 0 → 0 transition gains intensity and the 0 → 2 one becomes dominant, representing 48% of the total emission intensity (Table 5). In contrast, the contributions of the 0 → 1 and the 0 → 4 transitions decrease to 19% and 30%, respectively. The number of components of the 0 → 1 transition increases from two to three, and its total crystal-field splitting increases by about 100 cm^{-1} to become 278 cm^{-1} (Table 6). The distribution of intensity and the fine structure of the luminescence spectrum of **EuL2** in the solution (1, 3, >3, and >5 components for J = 0, 1, 2, 4) are not consistent with C_3-symmerty (which is observed in the solid), but point to a low C_1-symmetry around the metal ion (1, 3, 5, and 9 components predicted for J = 0, 1, 2, and 4).[3,17,23] The luminescence spectrum, however, reflects the presence of only one emitting Eu^{III} center in the solution (Figure 5 and Table 6).

The luminescence decays of **EuL1** and **EuL2** (τ_{obs}, Table 7) in the polycrystalline solid and in dichloromethane solution are single-exponential functions, again confirming the presence of one main emissive europium center in each case. The long luminescence lifetimes of 1.56−2.67 ms and the high ligand-sensitized luminescence quantum yields of 25−41% (Table 7)

Table 5. Relative Luminescence Intensity of $^5D_0 \rightarrow {}^7F_J$ Transitions of Europium Complexes[a]

complex		0→0	0→1	0→2	0→3	0→4	total/0→1
$[Eu(L1)_3]\cdot 4H_2O$	solid	0.005	1.00	1.36	0.16	1.57	4.10
$[Eu(L2)_3]\cdot 5H_2O$	solid	0.005	1.00	1.56	0.19	1.71	4.47
	CH_2Cl_2	0.02	1.00	2.60	0.15	1.63	5.40

[a]From Figure 5. Normalized to the $^5D_0 \rightarrow {}^7F_1$ transition. Integrated from the corrected luminescence spectra (photon/s) versus wavelength (nm) at 298 K at λ_{exc} = 355 nm. Estimated error: ±5%.

DOI: 10.1021/acs.inorgchem.5b01580
Inorg. Chem. XXXX, XXX, XXX−XXX

Table 6. Energies of ^7F_J and $^5D_0$ Levels of Europium Complexes[a]

complex		E/cm^{-1}					
		$^7F_0$	$^7F_1$	$^7F_2$	$^7F_3$	$^7F_4$	$^5D_0$
$[Eu(L1)_3]\cdot 4H_2O$	solid	0	275	997	1842	2718	17236
			446	1034 (sh)	1941	2760	
				1128	2015 (w)	2897	
						2950	
						3023	
$[Eu(L2)_3]\cdot 5H_2O$	solid	0	266	982	1833	2714	17232
			442	1129	1932	2901	
					2021 (w)	2967	
						3027	
	CH_2Cl_2	0	275	988	1883 (br)	2697	17253
			373	1067		2773	
			553	1186 (sh)		2832	
						2902	
						3053	

[a]From Figure 5. At 298 K. Estimated error: ±6 cm^{-1}.

Table 7. Luminescence Parameters of Europium Complexes[a]

complex		ν_{0-0}/cm^{-1}[b]	Q_L^{Eu}/%	τ_{obs}/ms		τ_{rad}/ms	Q_{Eu}^{Eu}/%	η_{sens}/%
				298 K	10 K			
$[Eu(L1)_3]\cdot 4H_2O$	solid	17236(9)	41	1.94	2.53	4.93	39	100
$[Eu(L2)_3]\cdot 5H_2O$	solid	17232(9)	25	1.56	2.67	4.52	35	71
	CH_2Cl_2		32	2.18		4.38	50	64

[a]At 298 K, unless stated otherwise. λ_{exc} = 355 nm. Relative errors: τ_{obs}, ±2%; Q_L^{Eu}, ±10%; τ_{rad}, ±10%; Q_{Eu}^{Eu}, ±12%; η_{sens}, ±22%. [b]From Figure 6. Full-width at half-height in parentheses.

indicate that water molecules are not coordinated to the europium in **EuL1** and **EuL2** in the solid and in solution.[17,31]

The luminescence lifetimes of the polycrystalline complexes increase significantly on cooling from 298 K to 10 K (but the luminescence decays remain single-exponential functions), especially for **EuL2**, pointing to the presence of a thermally activated nonradiative deactivation pathway. It may be caused by the europium-to-ligand back-transfer of energy,[28] because the energy gaps from the ligand triplet to the receiving levels Eu($^5D_1$) at 19 000 cm^{-1} and Eu($^5D_0$) at ~17 230 cm^{-1} are only 700−3170 cm^{-1}. Alternatively, it may be caused by quenching of Eu^{III} by a ligand-to-metal charge transfer (LMCT, a frequently observed process for electron-donating ligands[32]), especially for complex **EuL2**, with an electron-rich *n*-octyloxy-substituted ligand.

We have analyzed the photophysics of the complexes in terms of eq 3, where Q_L^{Eu} and Q_{Eu}^{Eu} are ligand-sensitized and intrinsic Eu($^5D_0$) luminescence quantum yields, η_{sens} is the efficiency of ligand-to-europium energy transfer, and τ_{obs} and τ_{rad} are the observed and radiative lifetimes of Eu($^5D_0$):

$$Q_L^{Eu} = \eta_{sens} \times Q_{Eu}^{Eu} = \eta_{sens} \times (\tau_{obs}/\tau_{rad}) \quad (3)$$

The radiative lifetime of Eu($^5D_0$) was calculated from eq 4,[33] where *n* is the refractive index (1.5 for the solid complexes or 1.4242 for the CH_2Cl_2 solution), $A_{0\to1}$ is the spontaneous emission probability for the $^5D_0 \to {}^7F_1$ transition in vacuo (14.65 s^{-1}), and $I_{tot}/I_{0\to1}$ is the ratio of the integrated emission intensity of the total corrected europium spectrum to that of the magnetic-dipole $^5D_0 \to {}^7F_1$ transition (Table 5):

$$1/\tau_{rad} = A_{0\to1} \times n^3 \times (I_{tot}/I_{0\to1}) \quad (4)$$

Table 7 reports the photophysical parameters. The radiative lifetimes of the solid complexes are 4.93 ms for **EuL1** and 4.52 ms for **EuL2**. When **EuL2** is dissolved in dichloromethane, one anticipates a lengthening of its τ_{rad} from 4.52 ms (in the solid) to 5.28 ms (in solution) due to the decrease in refractive index (eq 4),[1,2] provided that the coordination sphere of the europium ion remains the same. In the experiment, however, we observe a shortening of the radiative lifetime to 4.38 ms in dichloromethane, which indicates that the coordination sphere of the europium ion changes upon dissolution of **EuL2**, probably to give a lower symmetry environment.

The intrinsic quantum yield of europium could not be measured because of the low intensity of the f−f absorption. Instead, it was calculated from the ratio $Q_{Eu}^{Eu} = \tau_{obs}/\tau_{rad}$ to be 35−39% for the solid complexes and 50% for the **EuL2** solution. The higher Q_{Eu}^{Eu} in solution for **EuL2** results both from the longer τ_{obs} and from the shorter τ_{rad}.

In the solid complexes, the calculated efficiency of ligand-to-europium energy transfer, $\eta_{sens} = Q_L^{Eu}/Q_{Eu}^{Eu}$, decreases from 100% in **EuL1** to 71% in **EuL2**, because of the more facile nonradiative deactivation of **EuL2** both by energy back-transfer and by LMCT (see above). The sensitization efficiency for **EuL2** in solution (64%) is comparable to that in the solid (71%), indicating that the ligands remain bound to the europium in dichloromethane, a noncoordinating solvent.

The luminescence quantum yield and observed lifetime of **EuL2** increase in going from the solid to the solution, probably, in part, because the five cocrystallized water molecules in the solid **EuL2** quench the emissive state of europium via a second-sphere interaction. In contrast, in dichloromethane, these water molecules move into the bulk solution and are less likely to quench the europium ion.

DOI: 10.1021/acs.inorgchem.5b01580
Inorg. Chem. XXXX, XXX, XXX−XXX

Symmetry and Luminescence. The crystal structures reveal that the solid complexes **LnL1** have a rare C_3-symmetry of the lanthanide coordination polyhedron (Figure 2). The nearly identical luminescence spectra of the polycrystalline **EuL1** and **EuL2** suggest that the **LnL2** complexes in the solid have C_3-symmetry also (Figure 5). In fact, the luminescence spectra of the polycrystalline **EuL1** and **EuL2** are similar in intensity distribution and fine structure to those of the reference Eu^{III} complexes **R4**[23] and **R6**[2] (Chart 1) of C_3- or D_3-symmetry (in which the intensity of the 0 → 1 transition is comparable to that of the 0 → 2, while the 0 → 4 transition is the most intense), but are different from those of complexes **R1**[17] of C_1-symmetry (in which the 0 → 2 transition is the most intense).

The lanthanide−ligand bonds have predominant ionic character and, therefore, are nondirectional and labile, even with polydentate ligands.[2,34] The significant changes in the luminescence spectrum as well as the shortening of the radiative lifetime of **EuL2** in going from the solid state to dichloromethane solution indicate a modification in the coordination environment of the europium ion. For example, in sharp contrast to **EuL2**, the radiative lifetime of **R6**, which have pseudo-D_3-symmetry in all media, increases from 4.9 ms in the solid to 6.2−6.9 ms in aqueous solution due to the change in refractive index.[2]

We consider that in dichloromethane solution the labile lanthanide−ligand bonding lowers the symmetry of **EuL2** from C_3 to C_1 by modifying the arrangement of the three ligands from "up−up−up" to "up−up−down" (for example, see the C_1-crystal structures of **R1**[17]). Taking into account the spectroscopic data, a mixture of C_1- and C_3-species in solution can most probably be ruled out. The photophysical properties of **EuL2** are different in the solid but are similar in solution to those of the reference Eu^{III} complexes with C_1-symmetry. For example, for 16 complexes **R1**, which have C_1-symmetry in all media, the radiative lifetimes are 3.22−4.7 ms in the solid and often increase to 3.91−4.40 ms in dichloromethane solution, while the luminescence spectra do not change (apart from becoming broader in solution) and have three components for the 0 → 1 transition.[17] Moreover, the luminescence spectra of the C_1-symmetry complexes **R1**[17] and **R3**−**R5**[22−24] are dominated by the 0 → 2 transition.

It appears that the C_3- and C_1-symmetry species (isomers) for **EuL2** are close in energy and, because of the labile lanthanide−ligand bonding, easily interconvert. The isolation of a rare C_3-species in the solid state for **LnL1** and **LnL2** is probably driven by crystal packing of the *N*-benzyl groups (in contrast, the *N*-alkyl and *N*-aryl analogues **R1** have C_1-symmetry in all media[17]). The cocrystallized solvent does not seem to play a crucial role in determining the C_3-symmetry of the complex in the solid; for example, a molecule of acetonitrile is cocrystallized in the single crystal of $[La(\mathbf{L1})_3]\cdot CH_3CN$, but water molecules are cocrystallized in the polycrystalline $[Eu(\mathbf{L1})_3]\cdot 4H_2O$ and $[Eu(\mathbf{L2})_3]\cdot 5H_2O$. The conversion of C_3- to C_1-species of **EuL2** in going from the solid to the solution is probably driven by a gain in entropy on lowering of the symmetry.

We note previous reports on the isomerization of the *fac* and *mer* six-coordinate complexes $[LnCl_3(\text{hexamethylphosphoramide})_3]$[35] and of the C_3 and C_1 nine-coordinate complexes $[Ln(8\text{-hydroxyquinolinate-2-carboxylate})_3]^{3-}$ and **R9**[26] (Chart 1). The thermodynamics of the interconversion of C_3- and C_1-species in acetonitrile solution were studied for **R10** (Chart 1).[36] Two symmetry/structure isomers of eight-coordinate lanthanide complexes were crystallized for $[Ln(\beta\text{-diketonate O^O})_3(H_2O)_2]$[37] and $[Ln(\beta\text{-diketonate O^O})_3(\text{diimine N^N})]$[38] and were identified by X-ray structure analysis and by luminescence spectroscopy of the europium complexes.

Conclusions. We report on mononuclear nine-coordinate lanthanum(III) and europium(III) complexes $[Ln(N^\wedge N^\wedge O)_3]$ with a rare C_3-symmetry of the lanthanide coordination polyhedron in the solid. These complexes, however, exhibit a lower C_1-symmetry in dichloromethane solution.

The change of the luminescence spectrum and the shortening of the $Eu(^5D_0)$ radiative lifetime in going from the (higher) C_3- to the (lower) C_1-symmetry species of **EuL2** (Table 5) suggests that the lower is the symmetry, the more allowed are the forbidden f−f transitions, which is in line with the predictions made from group-theoretical considerations.[1−3]

The shorter is the radiative lifetime, in other words, the faster is the rate of the radiative transition, the better the nonradiative processes can compete with the nonradiative ones (provided that they are not changed), and, therefore, the higher is the luminescence efficiency,[1,2,32,39] which is what we observe for **EuL2** in going from the solid to the solution (Table 5).

Therefore, care has to be taken when comparing photophysical properties of a labile lanthanide complex in various media, because the coordination environment of a lanthanide ion can change its symmetry even without a change in its composition.

■ EXPERIMENTAL SECTION

General Information. Elemental analyses were performed by Dr. E. Solari, Service for Elemental Analysis, Institute of Chemical Sciences and Engineering (EPFL). ^{1}H NMR spectra were recorded on Bruker Avance DRX 400 MHz spectrometer. Absorption spectra were measured on a PerkinElmer Lambda 900 UV/vis/NIR spectrometer. Luminescence spectra were recorded on a Horiba-Jobin Yvon Fluorolog FL 3-22 spectrometer and were corrected for the instrumental function. Quantum yields were determined on the same instrument by an absolute method with a modified homemade integrating sphere. Luminescence lifetimes were measured with a previously described instrumental setup.[17] Reported luminescence quantum yields and lifetimes are an average of 3−6 independent determinations. Spectroscopic studies were conducted in optical cells of 2 mm path length or in 2 mm i.d. quartz capillaries under air. The solutions in CH_2Cl_2 (Fisher Scientific, analytical reagent grade) were freshly prepared before each experiment.

Commercial reagents were used without purification. Chromatography was performed on a column with an i.d. of 30 mm on silica gel 60 (Fluka, Nr 60752). The progress of reactions and the elution of products were followed on TLC plates (silica gel 60 F_{254} on aluminum sheets, Merck).

Synthesis of Ligands. The reaction was performed under air.[17,19] Substituted pyridine-2-carboxaldehyde (its synthesis is described in the Supporting Information) was dissolved in formic acid (Merck, 98−100%) at room temperature to give a yellow solution, which sometimes appeared cloudy because of the presence of a red solid, probably residual Se from the previous synthetic step. The amount of formic acid was a minimum of 3−5 molar equiv relative to aldehyde or the minimum volume necessary to dissolve the aldehyde at 0 °C. The solution was cooled to 0 °C and stirred for 10 min. Then, cold H_2O_2 (30% wt aqueous solution) was added in excess. The solution was stirred for 6 h at 0 °C and kept overnight at 0 °C. Addition of ice-cold water to the solution precipitated the product. The suspension was stirred for 1 h at 0 °C and filtered. The product was washed with water and organic solvent, and then it was dried under vacuum. Further details are provided below.

HL1·H_2O. Aldehyde L1-CHO (Supporting Information, 445 mg, 1.42 mmol), formic acid (3 mL, 3.66 g, 0.08 mol), and H_2O_2 (0.85 mL of a 30% wt aqueous solution containing 283 mg of H_2O_2, 8.32 mmol)

DOI: 10.1021/acs.inorgchem.5b01580
Inorg. Chem. XXXX, XXX, XXX−XXX

gave after precipitation with 10 mL of water and after washing with water, hexane, and a small volume of 1:1 hexane/ether a white solid: 436 mg (1.26 mmol, 88%). Anal. Calcd for $C_{20}H_{15}N_3O_2{\cdot}H_2O$ (MW 347.37): C, 69.15; H, 4.93; N, 12.10. Found: C, 69.14; H, 4.89; N, 11.77. ^{1}H NMR (400 MHz, DMSO-d_6): δ = 8.55 (dd, J = 7.6, 1.2 Hz, 1H), 8.19−8.08 (m, 2H), 7.78 (d, J = 7.2 Hz, 1H), 7.71 (d, J = 7.2 Hz, 1H), 7.36−7.25 (m, 2H), 7.24−7.12 (m, 5H), 6.40 (s, 2H) ppm; CO_2H proton was not observed. ESI$^-$ TOF MS: m/z 328.1 $\{M - H\}^-$.

HL2·0.5H$_2$O. Aldehyde L2-CHO (Supporting Information, 627 mg, 1.42 mmol), formic acid (4 mL, 4.88 g, 0.11 mol), and H_2O_2 (0.85 mL of a 30% wt aqueous solution containing 283 mg of H_2O_2, 8.32 mmol) gave after precipitation with 15 mL of water and after washing with water and hexane a pale pink solid: 565 mg (1.21 mmol, 85%). Anal. Calcd for $C_{28}H_{31}N_3O_3{\cdot}0.5H_2O$ (MW 466.57): C, 72.08; H, 6.91; N, 9.01. Found: C, 72.16; H, 6.89; N, 8.94. ^{1}H NMR (400 MHz, DMSO-d_6): δ = 8.46 (dd, J = 7.6, 1.6 Hz, 1H), 8.12−8.02 (m, 2H), 7.62 (d, J = 8.8 Hz, 1H), 7.22 (d, J = 2.0 Hz, 1H), 7.21−7.10 (m, 5H), 6.89 (dd, J = 8.8, 2.4 Hz, 1H), 6.34 (s, 2H), 3.99 (t, J = 6.8 Hz, 2H), 1.75−1.65 (m, 2H), 1.46−1.18 (m, 10H), 0.85 (t, J = 6.8 Hz, 3H) ppm; CO_2H proton not observed. ESI$^-$ TOF MS: m/z 456.2 $\{M - H\}^-$.

Synthesis of Complexes. The reaction was performed under air. The ligand was suspended in ethanol (5 mL), followed by addition of NaOH dissolved in water (used as a stock solution with approximately 100 mg of NaOH per 10 mL of water) and stirring for 5 min to give a solution. The solution was warmed to 70−80 °C. After 5 min of stirring, a solution of $LnCl_3{\cdot}nH_2O$ in water (2 mL) was added dropwise over 5 min (a white precipitate may form on addition). Water (1 mL for **LnL1** and **EuL2**; 2 mL for **LaL2**) was added to induce and complete precipitation of the complex. The suspension was stirred for 10 min at 70−80 °C, cooled to 40−50 °C, and filtered while warm (the strict control of time and temperature is not required in this synthesis). The product was washed with ethanol/water (1:1) and either ether (**LnL1**) or hexane (**LnL2**) in that order. The complexes were dried under vacuum at room temperature. All of the complexes are soluble in DMSO, hot ethanol, and hot acetonitrile and are insoluble in hexane, ether, and water. The complexes **LnL2** (but not **LnL1**) are soluble in dichloromethane. Further details are provided below.

[La(L1)$_3$]·4H$_2$O: white solid; 48 mg (0.040 mmol, 84%) from HL1·H_2O (50 mg, 0.144 mmol), NaOH (5.76 mg, 0.144 mmol), and $LaCl_3{\cdot}7H_2O$ (17.8 mg, 0.048 mmol). Anal. Calcd for $C_{60}H_{42}LaN_9O_6{\cdot}4H_2O$ (MW 1196.00): C, 60.25; H, 4.21; N, 10.54. Found: C, 60.32; H, 4.24; N, 10.26. ^{1}H NMR (400 MHz, DMSO-d_6, 373 K, [C] = 0.79 × 10^{-3} M; the complex dissociates in DMSO, a coordinating solvent): δ = 8.17 (d, J = 7.6 Hz, 3H), 8.00 (t, J = 7.6 Hz, 3H), 7.95 (d, J = 7.6 Hz, 3H), 7.87 (d, J = 8.0 Hz, 3H), 7.61 (d, J = 8.0 Hz, 3H), 7.29 (t, J = 7.6 Hz, 3H), 7.27−7.07 (m, 18H), 6.18 (s, 6H) ppm.

[Eu(L1)$_3$]·4H$_2$O: white solid; 49 mg (0.041 mmol, 84%) from HL1·H_2O (50 mg, 0.144 mmol), NaOH (5.76 mg, 0.144 mmol), and $EuCl_3{\cdot}6H_2O$ (17.5 mg, 0.048 mmol). Anal. Calcd for $C_{60}H_{42}EuN_9O_6{\cdot}4H_2O$ (MW 1209.06): C, 59.60; H, 4.17; N, 10.43. Found: C, 59.66; H, 4.34; N, 10.16.

[La(L2)$_3$]·4H$_2$O: pale pink solid; 43 mg (0.027 mmol, 78%) from HL2·0.5H_2O (50 mg, 0.107 mmol), NaOH (4.3 mg, 0.107 mmol), and $LaCl_3{\cdot}7H_2O$ (13.3 mg, 0.035 mmol). The ^{1}H NMR of the complex in CD_2Cl_2, a noncoordinating solvent, at room temperature was broad and noninformative. Anal. Calcd for $C_{84}H_{90}LaN_9O_9{\cdot}4H_2O$ (MW 1580.63): C, 63.83; H, 6.25; N, 7.98. Found: C, 63.73; H, 6.44; N, 7.79. ESI$^+$ TOF MS: m/z 1531.7 $\{M + Na\}^+$.

[Eu(L2)$_3$]·5H$_2$O: off-white solid; 44 mg (0.027 mmol, 78%) from HL2·0.5H_2O (50 mg, 0.107 mmol), NaOH (4.3 mg, 0.107 mmol), and $EuCl_3{\cdot}6H_2O$ (13.1 mg, 0.035 mmol). Anal. Calcd for $C_{84}H_{90}EuN_9O_9{\cdot}5H_2O$ (MW 1611.71): C, 62.60; H, 6.25; N, 7.82. Found: C, 62.64; H, 6.35; N, 7.63. ESI$^+$ TOF MS: m/z 1544.8 $\{M + Na\}^+$.

■ ASSOCIATED CONTENT

Supporting Information

The Supporting Information is available free of charge on the ACS Publications website at DOI: 10.1021/acs.inorgchem.5b01580.

Synthesis of precursors; excitation and emission spectra; ^{1}H NMR spectra; crystallographic data (PDF)

CIF for the crystal structure CCDC 1409902 (CIF)

■ AUTHOR INFORMATION

Corresponding Authors

*E-mail (N. M. Shavaleev): shava@mail.ru.

*E-mail (J.-C. G. Bünzli): jean-claude.bunzli@epfl.ch. Tel: +41 21 693 9821. Fax: +41 21 693 5550.

Notes

The authors declare no competing financial interest.

■ ACKNOWLEDGMENTS

This project was supported by the Swiss National Science Foundation (grant 200020_119866/1).

■ REFERENCES

(1) Bünzli, J.-C. G. *Coord. Chem. Rev.* **2015**, *293−294*, 19.

(2) Bünzli, J.-C. G.; Chauvin, A.-S.; Kim, H. K.; Deiters, E.; Eliseeva, S. V. *Coord. Chem. Rev.* **2010**, *254*, 2623 and references therein.

(3) (a) Tanner, P. A. *Chem. Soc. Rev.* **2013**, *42*, 5090. (b) Binnemans, K. *Coord. Chem. Rev.* **2015**, *295*, 1.

(4) Vicentini, G.; Zinner, L. B.; Zukerman-Schpector, J.; Zinner, K. *Coord. Chem. Rev.* **2000**, *196*, 353.

(5) (a) de Sá, G. F.; Malta, O. L.; de Mello Donegá, C.; Simas, A. M.; Longo, R. L.; Santa-Cruz, P. A.; da Silva, E. F., Jr. *Coord. Chem. Rev.* **2000**, *196*, 165. (b) Gawryszewska, P.; Sokolnicki, J.; Legendziewicz, J. *Coord. Chem. Rev.* **2005**, *249*, 2489. (c) Armelao, L.; Quici, S.; Barigelletti, F.; Accorsi, G.; Bottaro, G.; Cavazzini, M.; Tondello, E. *Coord. Chem. Rev.* **2010**, *254*, 487. (d) Ma, Y.; Wang, Y. *Coord. Chem. Rev.* **2010**, *254*, 972. (e) Reddy, M. L. P.; Sivakumar, S. *Dalton Trans.* **2013**, *42*, 2663. (f) de Bettencourt-Dias, A.; Barber, P. S.; Viswanathan, S. *Coord. Chem. Rev.* **2014**, *273−274*, 165. (g) Comby, S.; Surender, E. M.; Kotova, O.; Truman, L. K.; Molloy, J. K.; Gunnlaugsson, T. *Inorg. Chem.* **2014**, *53*, 1867.

(6) (a) Chen, F.; Bian, Z.; Huang, C. *J. Rare Earths* **2009**, *27*, 345. (b) Katkova, M. A.; Bochkarev, M. N. *Dalton Trans.* **2010**, *39*, 6599.

(7) van der Ende, B. M.; Aarts, L.; Meijerink, A. *Phys. Chem. Chem. Phys.* **2009**, *11*, 11081.

(8) Andres, J.; Hersch, R. D.; Moser, J.-E.; Chauvin, A.-S. *Adv. Funct. Mater.* **2014**, *24*, 5029.

(9) Darmanyan, A. P.; Lazorchak, N.; Jardon, P. *J. Photochem. Photobiol., A* **1991**, *58*, 185.

(10) (a) Sykes, D.; Tidmarsh, I. S.; Barbieri, A.; Sazanovich, I. V.; Weinstein, J. A.; Ward, M. D. *Inorg. Chem.* **2011**, *50*, 11323. (b) Caillé, F.; Bonnet, C. S.; Buron, F.; Villette, S.; Helm, L.; Petoud, S.; Suzenet, F.; Tóth, E. *Inorg. Chem.* **2012**, *51*, 2522. (c) Starck, M.; Ziessel, R. *Dalton Trans.* **2012**, *41*, 13298. (d) Fisher, C. M.; Fuller, E.; Burke, B. P.; Mogilireddy, V.; Pope, S. J. A.; Sparke, A. E.; Déchamps-Olivier, I.; Cadiou, C.; Chuburu, F.; Faulkner, S.; Archibald, S. J. *Dalton Trans.* **2014**, *43*, 9567. (e) Routledge, J. D.; Jones, M. W.; Faulkner, S.; Tropiano, M. *Inorg. Chem.* **2015**, *54*, 3337. (f) Placide, V.; Bui, A. T.; Grichine, A.; Duperray, A.; Pitrat, D.; Andraud, C.; Maury, O. *Dalton Trans.* **2015**, *44*, 4918. (g) Guanci, C.; Giovenzana, G.; Lattuada, L.; Platas-Iglesias, C.; Charbonnière, L. J. *Dalton Trans.* **2015**, *44*, 7654.

(11) Nakamura, K.; Hasegawa, Y.; Kawai, H.; Yasuda, N.; Kanehisa, N.; Kai, Y.; Nagamura, T.; Yanagida, S.; Wada, Y. *J. Phys. Chem. A* **2007**, *111*, 3029.

(12) Bortoluzzi, M.; Paolucci, G.; Polizzi, S.; Bellotto, L.; Enrichi, F.; Ciorba, S.; Richards, B. S. *Inorg. Chem. Commun.* **2011**, *14*, 1762.

DOI: 10.1021/acs.inorgchem.5b01580
Inorg. Chem. XXXX, XXX, XXX−XXX

(13) Akerboom, S.; van den Elshout, J. J. M. H.; Mutikainen, I.; Siegler, M. A.; Fu, W. T.; Bouwman, E. *Eur. J. Inorg. Chem.* **2013**, 6137.
(14) (a) Blasse, G. *Chem. Phys. Lett.* **1973**, *20*, 573. (b) Reisfeld, R.; Zigansky, E.; Gaft, M. *Mol. Phys.* **2004**, *102*, 1319.
(15) (a) Kirby, A. F.; Foster, D.; Richardson, F. S. *Chem. Phys. Lett.* **1983**, *95*, 507. (b) Thompson, L. C.; Kuo, S. C. *Inorg. Chim. Acta* **1988**, *149*, 305.
(16) Piguet, C.; Bocquet, B.; Hopfgartner, G. *Helv. Chim. Acta* **1994**, *77*, 931.
(17) Shavaleev, N. M.; Eliseeva, S. V.; Scopelliti, R.; Bünzli, J.-C. G. *Inorg. Chem.* **2010**, *49*, 3927 and references therein.
(18) Yang, D. L.; Fokas, D.; Li, J. Z.; Yu, L. B.; Baldino, C. M. *Synthesis* **2005**, 47.
(19) Dodd, R.; Le Hyaric, M. *Synthesis* **1993**, *1993*, 295.
(20) Brown, I. D.; Altermatt, D. *Acta Crystallogr., Sect. B: Struct. Sci.* **1985**, *41*, 244.
(21) (a) Trzesowska, A.; Kruszynski, R.; Bartczak, T. J. *Acta Crystallogr., Sect. B: Struct. Sci.* **2004**, *60*, 174. (b) Trzesowska, A.; Kruszynski, R.; Bartczak, T. J. *Acta Crystallogr., Sect. B: Struct. Sci.* **2005**, *61*, 429.
(22) (a) Kottas, G. S.; Mehlstäubl, M.; Fröhlich, R.; De Cola, L. *Eur. J. Inorg. Chem.* **2007**, 3465. (b) Botelho, M. B. S.; Gálvez-López, M. D.; De Cola, L.; Albuquerque, R. Q.; de Camargo, A. S. S. *Eur. J. Inorg. Chem.* **2013**, 5064.
(23) Yamauchi, S.; Hashibe, T.; Murase, M.; Hagiwara, H.; Matsumoto, N.; Tsuchimoto, M. *Polyhedron* **2013**, *49*, 105.
(24) Andreiadis, E. S.; Imbert, D.; Pécaut, J.; Demadrille, R.; Mazzanti, M. *Dalton Trans.* **2012**, *41*, 1268.
(25) Wei, H.; Yu, G.; Zhao, Z.; Liu, Z.; Bian, Z.; Huang, C. *Dalton Trans.* **2013**, *42*, 8951.
(26) Bozoklu, G.; Marchal, C.; Pécaut, J.; Imbert, D.; Mazzanti, M. *Dalton Trans.* **2010**, *39*, 9112.
(27) (a) Crosby, G. A.; Whan, R. E. *J. Chem. Phys.* **1960**, *32*, 614. (b) Crosby, G. A.; Whan, R. E. *J. Chem. Phys.* **1962**, *36*, 863.
(28) Latva, M.; Takalo, H.; Mukkala, V. M.; Matachescu, C.; Rodríguez-Ubis, J. C.; Kankare, J. *J. Lumin.* **1997**, *75*, 149.
(29) Carnall, W. T.; Fields, P. R.; Rajnak, K. *J. Chem. Phys.* **1968**, *49*, 4450.
(30) Walton, J. W.; Carr, R.; Evans, N. H.; Funk, A. M.; Kenwright, A. M.; Parker, D.; Yufit, D. S.; Botta, M.; De Pinto, S.; Wong, K.-L. *Inorg. Chem.* **2012**, *51*, 8042.
(31) (a) Beeby, A.; Clarkson, I. M.; Dickins, R. S.; Faulkner, S.; Parker, D.; Royle, L.; de Sousa, A. S.; Williams, J. A. G.; Woods, M. *J. Chem. Soc., Perkin Trans. 2* **1999**, 493. (b) Supkowski, R. M.; Horrocks, W. DeW., Jr. *Inorg. Chim. Acta* **2002**, *340*, 44.
(32) Napier, G. D. R.; Neilson, J. D.; Shepherd, T. M. *Chem. Phys. Lett.* **1975**, *31*, 328.
(33) (a) Werts, M. H. V.; Jukes, R. T. F.; Verhoeven, J. W. *Phys. Chem. Chem. Phys.* **2002**, *4*, 1542. (b) Aebischer, A.; Gumy, F.; Bünzli, J.-C. G. *Phys. Chem. Chem. Phys.* **2009**, *11*, 1346.
(34) Bhaumik, M. L. *J. Inorg. Nucl. Chem.* **1965**, *27*, 243.
(35) Petriček, S.; Demšar, A.; Golič, L.; Košmrlj, J. *Polyhedron* **2000**, *19*, 199.
(36) Le Borgne, T.; Altmann, P.; André, N.; Bünzli, J.-C. G.; Bernardinelli, G.; Morgantini, P.-Y.; Weber, J.; Piguet, C. *Dalton Trans.* **2004**, 723.
(37) Nakamura, M.; Nakamura, R.; Nagai, K.; Shimoi, M.; Tomoda, S.; Takeuchi, Y.; Ouchi, A. *Bull. Chem. Soc. Jpn.* **1986**, *59*, 332.
(38) (a) Holz, R. C.; Thompson, L. C. *Inorg. Chem.* **1993**, *32*, 5251. (b) Thompson, L. C.; Atchison, F. W.; Young, V. G. *J. Alloys Compd.* **1998**, *275–277*, 765.
(39) Doffek, C.; Seitz, M. *Angew. Chem., Int. Ed.* **2015**, *54*, 9719.

DOI: 10.1021/acs.inorgchem.5b01580
Inorg. Chem. XXXX, XXX, XXX−XXX